University of Wisconsin - Madison

MADPH-99-1106
FSU-HEP-990419
April 1999

NLO QCD predictions for internal jet shapes in DIS at HERA

N. Kauer[1], L. Reina[2], J. Repond[3], and D. Zeppenfeld[1]

[1]*Department of Physics, University of Wisconsin, Madison, WI 53706*
[2]*Department of Physics, Florida State University, Tallahassee, FL 32306*
[3]*Argonne National Laboratory, Argonne, IL 60439*

Abstract

The transverse momentum flow inside jets is a sensitive measure of internal jet structure. For the current jets in deep inelastic scattering this jet shape measure is determined at order α_s^2, i.e. with up to three partons inside a single jet. The scale dependence of jet shapes in various jet algorithms is discussed. Results agree well with recent measurements by the ZEUS Collaboration, without introducing the hadronization parameter R_{sep}.

Experiments at the high energy frontier require a good understanding of jets, their distribution in phase space with respect to each other and to the leptons and photons produced in mixed electroweak-QCD processes. The internal structure of jets is equally important. Internal jet structure is intimately related to the number of jets reconstructed by different jet-defining algorithms. It also is an issue in reconstructing the kinematic properties of single jets, such as their transverse momentum or direction, and the invariant mass of two- or three-jet systems. Both aspects are important when searching for signs of new physics in hadron collider experiments.

One measure of internal jet structure is the transverse energy flow inside jets. This internal jet shape is defined as the fraction of a jet's transverse energy, E_T, which is deposited inside a sub-cone of radius $r < R$, where R is the cone size of the jet in the η-ϕ plane. Such jet shape measurements have been performed in the past at $p\bar{p}$ colliders [1,2] and also in photo-production and deep-inelastic-scattering (DIS) events at HERA [3–5], and have been compared to theoretical calculations [6–9]. Comparisons of the shape of gluon-rich jets at hadron colliders with the quark-dominated jets produced in ep and e^+e^- collisions [10] confirm the broader structure of gluon jets, which is expected because the larger color charge of gluons as compared to quarks leads to enhanced collinear radiation.

A major obstacle for a precise comparison of jet shape data to perturbative QCD predictions is the fact that, at tree level, QCD jets are single, massless partons. Hence, a nontrivial jet shape only arises at higher order, where a jet may contain two or more partons. Two partons inside a jet, which appear in typical NLO cross section calculations, produce jet shapes at lowest order only. Jets with three partons first appear in two-loop calculations and thus a determination of jet shapes at true NLO, in a given physical process, is extremely demanding theoretically. Photo-production of jets [7] or dijet production at the Tevatron [6] is a case in point: the kinematics of the event requires at least two hard jets in the final state, with balancing transverse momentum. A NLO jet shape, with jets consisting of three partons, thus requires four-parton final states at tree level and one-loop corrections to all $2 \to 3$ processes involving quarks and gluons. These corrections are only now becoming available [11].

In this letter we perform a full NLO jet shape calculation in a kinematically simpler situation: DIS at HERA. At sufficiently large Q^2, the scattered electron or positron in a DIS event provides the transverse momentum which is required to balance a high-E_T jet. A three-parton final state then suffices to generate jets containing three colored partons. The soft and collinear divergences, which are generated by integrating the three-parton contributions over the entire phase space, are canceled by one-loop corrections to two-parton final states and two-loop corrections to one-parton contributions. However, a single parton cannot produce internal jet structure and thus all true two-loop effects can be neglected when determining differential jet shapes for up to three partons. The full one-loop QCD corrections for two- and three-parton final states in DIS are implemented in the MEPJET Monte Carlo program [12]. Consequently, it is possible to extract full NLO jet shapes for the current jet in DIS with MEPJET.

In the following, we analyze NLO corrections to the differential jet shape $\rho(r, R, E_{Tj}, \eta_j)$ for events with a single jet of transverse energy E_{Tj} and pseudo-rapidity η_j. The differential jet shape is defined as

$$\rho(r, R, E_{Tj}, \eta_j) = \frac{1}{d^2\sigma_{NLO}/dE_{Tj}\, d\eta_j} \sum_n \int dr_n \, \frac{E_{Tn}}{E_{Tj}} \delta(r - r_n) \frac{d^3\sigma}{dE_{Tj}\, d\eta_j\, dr_n} \, . \tag{1}$$

Here the sum runs over all partons, n, belonging to the jet, which have a separation $r_n =$

$\sqrt{(\eta_n - \eta_j)^2 + (\phi_n - \phi_j)^2} = r < R$ from the axis of the jet in the legoplot. In practice, both the data and the Monte Carlo calculation replace the differential distributions by integrals over finite bin sizes in E_{Tj}, η_j and r. Since we want to compare our NLO results with the ZEUS data, we follow the ZEUS event selection [5] and study current jets in neutral current (NC) DIS events with

$$E_e > 10 \text{ GeV} , \qquad Q^2 > 100 \text{ GeV}^2 , \qquad E_{Tj} > 14 \text{ GeV} , \qquad -1 < \eta_j < 2 , \tag{2}$$

where E_e is the energy of the scattered electron in the laboratory frame. The default jet cone size is $R = 1$ and cone slices of width $\Delta r = 0.1$ are considered. Because of the modest jet E_T, b-quarks are unlikely to appear inside a current jet. Production of massive $\bar{b}b$ pairs via photon-gluon fusion is small also, for the cuts considered below. Thus it is appropriate to perform the calculations in a fixed 4-flavor scheme, neglecting any b-quark contributions. Matching 4-flavor parton distributions are provided by the CTEQ4F4 set [13]; for consistency with the parton distribution functions we use two-loop expressions for the running strong coupling constant, with $\Lambda^{(4)}_{\overline{\text{MS}}} = 292$ MeV.

For the theoretical jet shapes, the factors in the denominator of Eq. (1) are determined using NLO DIS cross sections at $\mathcal{O}(\alpha_s)$, within a given set of selection cuts. Therefore, they correspond to 1-jet exclusive cross sections for the 1-jet cuts described below. For the ZEUS cuts, 2-jet events also enter with single weight only. The numerator is determined at full $\mathcal{O}(\alpha_s^2)$ for the NLO results and at $\mathcal{O}(\alpha_s)$ for the LO calculations. The default version of the MEPJET2.2 program is written for the calculation of NLO dijet cross sections in DIS, i.e. allowing for one soft or collinear parton in the final state. For the calculation of jet shapes at NLO, up to two soft and/or collinear partons must be generated. We have modified the MEPJET phase space generator to cover this enlarged phase space region for two- and three-parton final states.

The matrix elements needed for the calculation of NLO jet shapes are identical to the ones used for the NLO dijet cross section and have been tested previously [12,14]. The cancellation of collinear and infrared singularities employs the phase space slicing method of Giele, Glover, and Kosower [15], which removes soft and/or collinear regions of the three-parton phase space, where some pair of final and/or initial parton momenta satisfies $2p_i \cdot p_j < s_{min}$. Contributions from these regions are approximated by the appropriate asymptotic expressions and added analytically to the two-parton contributions, where they cancel the soft and collinear singularities of the virtual contributions. The final result must be independent of the choice of s_{min}, for values of this soft cutoff sufficiently small to make the asymptotic approximations valid.

Numerical s_{min} independence is a powerful test for the correct implementation of observables and of the phase space generator, as well as for the infrared stability of the jet clustering algorithms [11]. Results of this s_{min} test are shown in Fig. 1 for the differential jet shapes at $r = 0.15$, 0.45, 0.65, and 0.95 in the successive combination algorithm of Ellis and Soper [16] (see below). Within Monte Carlo statistical errors of about 1-5%, results are independent of s_{min} below $s_{min} \approx 0.01$ GeV^2. We have checked that similar results hold for our implementation of the PUCELL jet algorithm employed by ZEUS [4]. We will use $s_{min} = 0.01$ GeV^2 in the following.

In our NLO calculation of jet shapes, the current jet contains up to three partons, which provides a much more detailed simulation of internal jet structure than is possible in a LO analysis. The extra detail suggests a direct comparison of NLO theory with data, with the E_T flow of hadrons in the data replaced by parton E_T. Previous LO analyses modeled hadronization

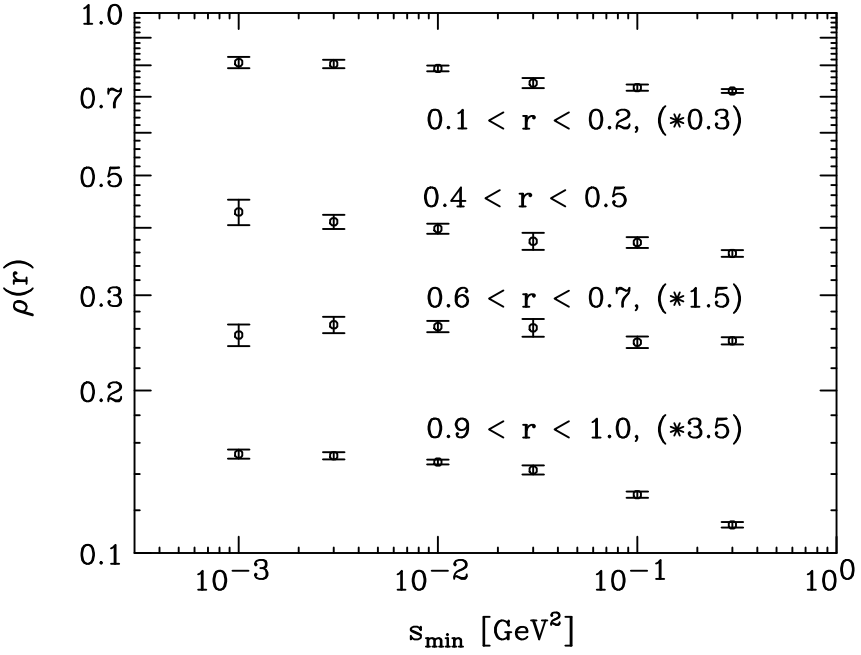

FIG. 1. s_{min} dependence of jet shapes $\rho(r)$ in four representative r-bins. The Ellis-Soper k_T algorithm [16] has been used, within the cuts of Eqs. (2,7) and requiring that only one hard jet, of $E_{Tj} > 5$ GeV is seen in the pseudo-rapidity range $-2.5 < \eta_j < 2.5$. Errors represent Monte Carlo statistics only. Note that results in three of the four bins have been rescaled by the factors given in parentheses.

effects by introducing a phenomenological parameter, R_{sep}, which controlled the clustering of partons with legoplot separations between R and $2R$ [17]. Our analysis implements the full experimental jet algorithms at the parton level, without introducing extra, tunable parameters. We have studied two algorithms in detail, the successive combination algorithm of Ellis and Soper [16], called k_T algorithm in the following, and the PUCELL algorithm used by the ZEUS Collaboration [4,5], for default cone sizes of $R = 1$.

The k_T algorithm successively combines pairs of nearest partons/protojets to new protojets, up to a distance R in the legoplot. Initially all partons are classified as protojets of transverse energy $E_T = p_T$. The algorithm then compares the E_T's of protojets, via $d_i = E_{Ti}R$, with the E_T weighted distances, $d_{ij} = \min(E_{Ti}, E_{Tj})\sqrt{(\eta_i - \eta_j)^2 + (\phi_i - \phi_j)^2}$, of pairs of protojets in the legoplot. The pair of protojets with the smallest d_{ij} is recombined if d_{ij} is smaller than all the d_i (which implies that their distance in the legoplot is smaller than R). Otherwise the protojet with the smallest E_T, and hence the smallest d_i, is called a jet and eliminated from the list of protojets. This process is iterated until all protojets have been assigned to jets. Note that some of these jets may be eliminated by subsequent selection cuts, as in Eq. (2). Some freedom exists in the assignment of jet momenta, i.e. in the recombination scheme. For the k_T algorithm we use the E-scheme, i.e. the jet four-momentum is the sum of the four-momenta of the partons belonging to the jet and the jet E_T is the sum of the parton p_T's. Apart from the definition of recombined momenta, our k_T algorithm is identical to the ones described in Refs. [9,16].

The PUCELL algorithm is an iterative fixed cone algorithm. In a first step all partons with $p_T > 300$ MeV are considered as seeds for the formation of pre-clusters. Starting with the highest p_T seed, a pre-cluster is formed, containing this seed and all seeds within a cone of radius

R around it. This procedure is iterated with the remaining seeds, which do not yet belong to a pre-cluster, in order of decreasing p_T. All the seeds belonging to a given pre-cluster are then merged, according to the Snowmass convention [18], i.e., the legoplot variables of the pre-clusters are defined as the E_T-weighted averages over the seeds,

$$E_{T,p.c.} = \sum_i E_{Ti} \ , \tag{3}$$

$$\eta_{p.c.} = \frac{1}{E_{T,p.c.}} \sum_i E_{Ti} \, \eta_i \ , \tag{4}$$

$$\phi_{p.c.} = \frac{1}{E_{T,p.c.}} \sum_i E_{Ti} \, \phi_i \ . \tag{5}$$

In a second step, all partons are considered, even if they fall below the seed threshold of 300 MeV. A new cluster axis is calculated as in (3-5), in terms of all partons inside a cone of radius R of the old (pre)cluster axis. This second step is iterated until the contents of all clusters stabilize. A third step deals with overlapping clusters, i.e. with clusters which share partons. If the energy of the common partons is more than 75% of the energy of the lower-energy cluster, the two clusters are merged to a single jet. Otherwise two separate jets are formed and common partons are assigned to the nearest jet.

We can now compare the jet shape predictions for these jet algorithms at both leading and next-to-leading order. One way to assess the improvements from a NLO calculation is to study the scale dependence of observables. The process at hand is inclusive DIS which basically has a single scale only, Q, the momentum transfer carried by the virtual photon. Q is the obvious choice for the factorization scale and we fix $\mu_f^2 = Q^2$ throughout. On the other hand, we are investigating the inner structure of jets, and the average jet mass or the average transverse momentum of partons, with respect to the jet axis, appear as reasonable scale choices[1]. These scales are proportional to the intrinsic scale of the entire process, Q, and become different from zero only at $\mathcal{O}(\alpha_s)$, thus suggesting $\alpha_s Q^2$ as a scale choice. This leads us to investigate variations of the renormalization scale $\mu_r^2 = \xi \alpha_s(Q^2) Q^2$ with the scale factor ξ. Searching for minimal sensitivity [19] of $\rho(r)$, a "correct" scale $\mu_r = Q$ would appear as a flat ξ-dependence near $\xi = 1/\alpha_s$. Thus, for all practical purposes, our choice is general enough. For the PUCELL algorithm and two representative bins in r, the scale variation of the differential jet shape, $\rho(r)$, is shown in Fig. 2.

The dash-dotted and dashed lines show the LO and NLO results for the generic ZEUS acceptance cuts of Eq. (2). The E_T flow is somewhat higher at NLO, i.e. jets are broader. However, the renormalization scale dependence is almost as large at NLO as for the LO case. This disappointing result can be traced to a large contribution from events with an additional low E_T jet. In DIS events with two jets, at $\mathcal{O}(\alpha_s^2)$, at best one jet can contain two partons, and, hence, the jet shape is modeled at LO only. In order to enhance the contribution from jets with the maximal number of partons, which then are truly modeled at NLO, events which contain additional jets should be eliminated. We achieve this goal by vetoing events containing any additional jets with

[1]The mass of the jet in an individual event appears as an integration variable in the determination of $\rho(r)$ and is not a physical scale of the observable.

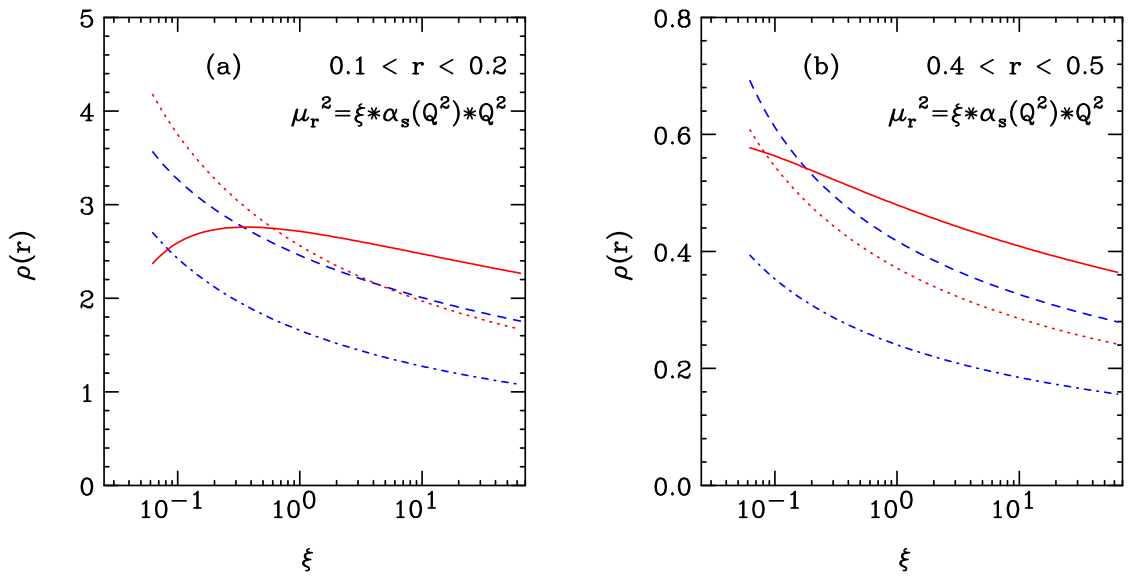

FIG. 2. Renormalization scale dependence of the differential jet shape $\rho(r)$ at (a) $r = 0.15$ and (b) $r = 0.45$, using the PUCELL algorithm. The dash-dotted and dashed lines are the LO and NLO results for the acceptance cuts of Eq. (2). Also shown are LO (dotted line) and NLO (solid line) results for events with one single jet only of $E_T > 5$ GeV (see Eqs. (6,7)).

$$E_{Tj} > 5 \text{ GeV} , \qquad -2.5 < \eta_j < 2.5 . \tag{6}$$

These veto cuts are chosen such that they can be easily implemented experimentally. A further reduction of events with hadronic activity beyond the current jet is achieved by requiring the scattered lepton and the observed hard jet to be back-to-back in azimuth. Allowing for finite detector resolution we require

$$\Delta\phi_{ej} = |\phi_e - \phi_j| > 3 . \tag{7}$$

Also shown in Fig. 2 is the scale dependence of $\rho(r)$ for events with the jet veto cut of Eq. (6) and the back-to-back cut of Eq. (7). In the following we call these restrictions "1-jet cuts". For these 1-jet events the scale independence of $\rho(r)$ is significantly improved at NLO, out to distances of $r \approx 0.6$.

The factors in the denominator of Eq. (1) are very stable against scale variations for inclusive DIS events, i.e. within the ZEUS cuts of Eq. (2). The 1-jet cuts, however, lead to a sizable reduction of $d^2\sigma_{NLO}/dE_{Tj}\,d\eta_j$ in the denominator of Eq. (1), corresponding to a subtraction of two-parton final states with dijet-type kinematics. This subtraction term is modeled at leading order only and is strongly scale dependent. However, it can be calculated at $\mathcal{O}(\alpha_s^2)$ also, which results in a more reliable determination. For the 1-jet cuts we find minimal scale sensitivity [19] near $\mu_r^2 = \alpha_s(Q^2)Q^2$, and at this value the $\mathcal{O}(\alpha_s)$ and $\mathcal{O}(\alpha_s^2)$ results for the subtraction terms virtually agree. We therefore use $\mu_r^2 = \alpha_s(Q^2)Q^2$ in the denominator, which increases the normalization of the resulting jet shapes by 10-15% as compared to the choice $\mu_r = Q$.

The renormalization scale dependences of jet shapes in the PUCELL and the k_T algorithm are compared in Fig. 3, using the 1-jet cuts. Results are shown for four representative r-bins,

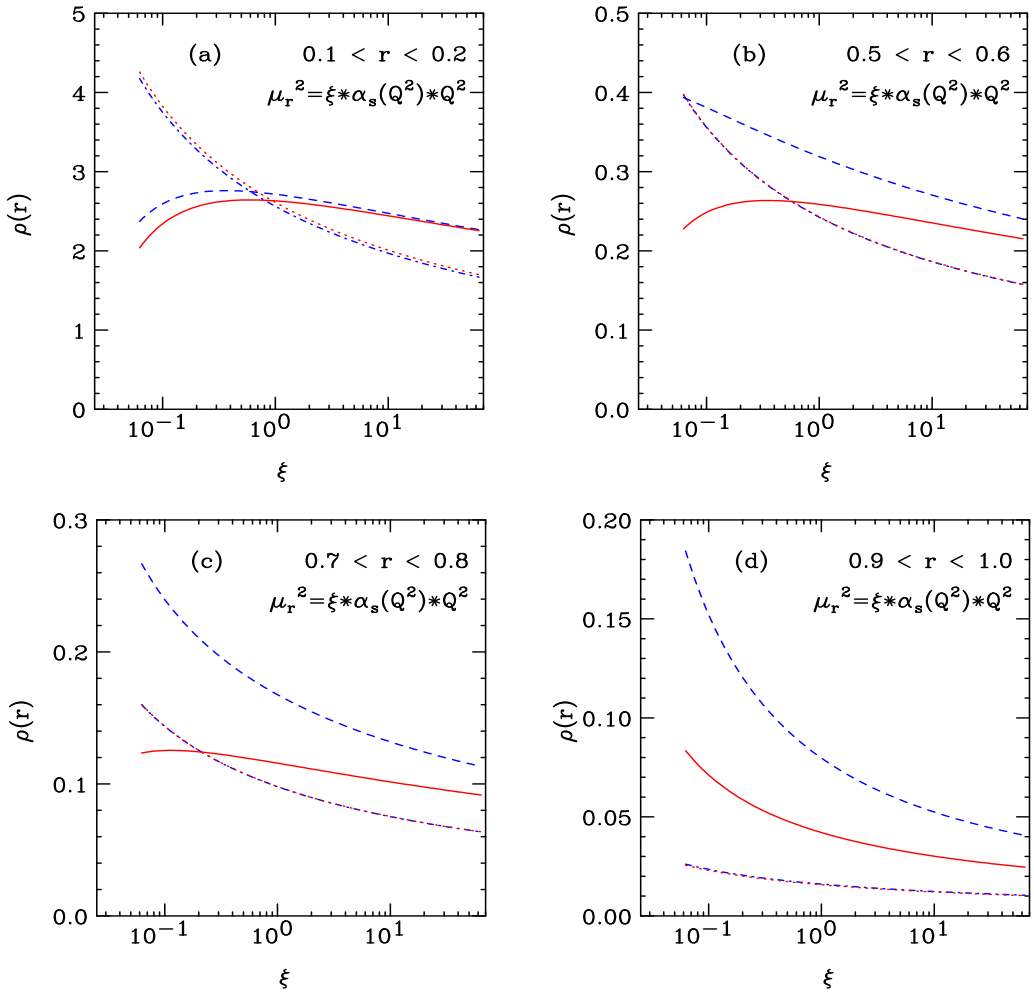

FIG. 3. Renormalization scale dependence of the differential jet shape $\rho(r)$ at (a) $r = 0.15$, (b) $r = 0.55$, (c) $r = 0.75$, and (d) $r = 0.95$, for events satisfying the 1-jet cuts of Eqs. (6,7). Results are shown for the PUCELL algorithm at LO (dash-dotted line) and NLO (dashed line) and for the k_T algorithm at LO (dotted line) and NLO (solid line).

at LO (dash-dotted and dotted lines) and at NLO (dashed and solid lines). The LO curves are virtually identical for the two algorithms. This is to be expected, since the criterion for merging two partons is the same at LO, namely their separation in the legoplot must be less than $R = 1$. Small differences are either statistical or due to the different recombination schemes for parton momenta. At NLO, the PUCELL and the k_T algorithm produce quite similar results for the central part of the jet (at small r). In this region, sensitivity to the choice of renormalization scale is minimal near $\xi = 1$ which confirms our basic choice of $\mu_r^2 = \alpha_s Q^2$. At distances from the jet axis beyond $r \approx 0.5$, the iterative nature of the PUCELL algorithm is more likely to gather a third parton into the jet, making it somewhat broader on average than jets reconstructed by the k_T algorithm. Since this broadening effect requires three partons and is therefore only modeled at tree level in our NLO calculation, the NLO enhancement of $\rho(r)$ at large r shows a pronounced scale dependence, which is significantly stronger in the PUCELL than in the k_T algorithm.

Differential jet shapes in DIS, as a function of E_T and pseudo-rapidity of the jet, have been measured by ZEUS [5]. In Fig. 4(a) we compare our LO and NLO QCD predictions with the ZEUS measurements for events with at least one hard jet. This jet is identified with the PUCELL algorithm and must lie in the interval 14 GeV $< E_T <$ 21 GeV and $-1 < \eta < 2$. The agreement

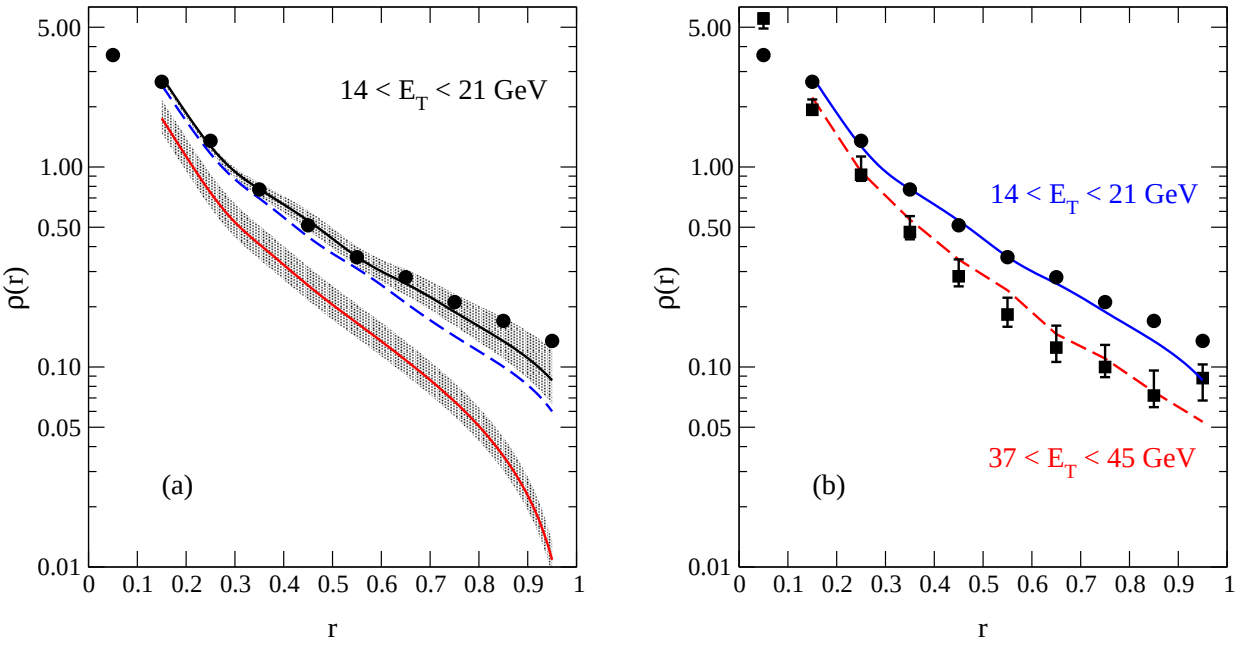

FIG. 4. Comparison of ZEUS jet shape data [5] with QCD predictions for DIS jets reconstructed by the PUCELL algorithm. Jet cuts are: $-1 < \eta < 2$ and (a,b) 14 GeV $< E_T <$ 21 GeV, (b) 37 GeV $< E_T <$ 45 GeV. ZEUS data (circles and squares) are compared in the lower E_T range (a) with LO (lower band) and NLO (dashed line) QCD predictions. The upper band in (a) and the two lines in (b) represent NLO jet shapes within the 1-jet cuts of Eqs. (6,7). The width of the bands corresponds to varying the renormalization scale between $\mu_r^2 = \alpha_s Q^2/4$ and $\mu_r^2 = 4\alpha_s Q^2$.

between data and theory in the $0.1 < r < 1$ range is improved significantly at NLO. Calculation of the jet shape at $r = 0$ is currently not possible, since it would require the inclusion of two-loop contributions and the resummation of multiple soft and collinear emission. As discussed previously, the scale dependence of the NLO results is quite large within the ZEUS acceptance cuts. The ZEUS data (and our NLO simulations) show, on the other hand, that the jet shapes depend very little on the jet pseudo-rapidity, and modestly on jet E_T. Imposing the 1-jet cuts of Eqs. (6,7) does not significantly change $\rho(r)$ for the default scale choice of $\mu_r^2 = \alpha_s Q^2$, but it reduces the scale uncertainty. Included in Fig. 4 are the NLO results using the 1-jet cuts. The NLO QCD predictions for $\rho(r)$ agree very well with the data, up to values around $r \approx 0.8$ for the 1-jet cuts and $r \approx 0.6$ for the generic ZEUS cuts. This corresponds to the regions where we have found a small scale dependence. In other words, the differences between data and NLO QCD are consistent with higher order QCD effects. Note that the agreement between theory and data is much worse at LO.

Similar agreement between true NLO QCD and ZEUS data is found for different jet E_T and η ranges. One example is shown in Fig. 4(b), where jet shapes for jets with 14 GeV $< E_T <$ 21 GeV and 37 GeV $< E_T <$ 45 GeV are compared. The data and the NLO QCD predictions clearly show that higher E_T jets are narrower. It should be noted that the excellent agreement between data and theory, at the 10% level, is obtained only when applying the minimal sensitivity criteria [19] to pick the renormalization scale. A naïve choice, like $\mu_r = Q$ (roughly corresponding to $\xi \approx 10$ in Fig. 3) would lead to substantially larger deviations from the experimental results.

We have performed a first analysis of true NLO jet shapes in DIS. We find excellent agreement between NLO QCD and data. This agreement is achieved without introducing extra phenomenological parameters describing hadronization effects, like R_{sep}. For the PUCELL and the k_T algorithm we have shown that the scale uncertainty of the QCD predictions for jet shapes is substantially reduced at NLO. A precise comparison of experiment with theory is facilitated by cuts which suppress multi-jet events. Our analysis can be easily extended to other jet algorithms and momentum recombination schemes and allows one to investigate questions like the infrared safety of jet algorithms or the reconstruction of kinematical variables from jets at full NLO. Their effect on the matching of theory and data for ep collisions at HERA and more generally at hadron colliders can now be investigated at the one-loop level.

ACKNOWLEDGMENTS

This research was supported in part by the University of Wisconsin Research Committee with funds granted by the Wisconsin Alumni Research Foundation and in part by the U. S. Department of Energy under Contract No. DE-FG02-95ER40896.

REFERENCES

[1] UA1 Collaboration, C. Albajar et al., Nucl. Phys. **B309** (1988) 405.

[2] CDF Collaboration, F. Abe et al., Phys. Rev. Lett. **70**, 713 (1993); D0 Collaboration, S. Abachi et al., Phys. Lett. **B357**, 500 (1995).

[3] H1 Collaboration, S. Aid et al., Z. Phys. **C70** (1996) 17.

[4] ZEUS Collaboration, J. Breitweg et al., Eur.Phys.J. **C2**, 61 (1998), [hep-ex/9710002].

[5] ZEUS Collaboration, J. Breitweg et al., preprint DESY-98-038 (1998), [hep-ex/9804001].

[6] S.D. Ellis, Z. Kunszt, D.E. Soper, Phys. Rev. Lett. **69** (1992) 3615.

[7] G. Kramer, S.G. Salesch, Phys. Lett. **B317** (1993) 218, Phys. Lett. **B333** (1994) 519; M. Klasen and G. Kramer, Phys. Rev. **D56**, 2702 (1997).

[8] W.T. Giele, E.W.N. Glover, and D.A. Kosower, Phys. Rev. **D57**, 1878 (1998).

[9] M.H. Seymour, Nucl. Phys. **B513**, 269 (1998).

[10] OPAL Collaboration, R. Akers et al., Z. Phys. **C63**, 197 (1994).

[11] Z. Bern, L. Dixon, and D.A. Kosower, Ann. Rev. Nucl. Part. Sci. **46**, 109 (1996) [hep-ph/9602280]; W.B. Kilgore and W.T. Giele, Phys. Rev. **D55**, 7183 (1997); W.B. Kilgore and W.T. Giele, *Hadronic three jet production at next-to-leading order*, e-Print hep-ph/9903361.

[12] E. Mirkes and D. Zeppenfeld, Phys. Lett. **B380**, 205 (1996); E. Mirkes, preprint TTP-97-39 (1997) [hep-ph/9711224].

[13] H. L. Lai and W. K. Tung, Z. Phys. **C74** (1997) 463, [hep-ph/9701256].

[14] D. Graudenz, e-Print Archive hep-ph/9710244.

[15] W. T. Giele and E. W. N. Glover, Phys. Rev. D **46** (1992) 1980; W. T. Giele, E. W. N. Glover and D.A. Kosower, Nucl. Phys. **B403** (1993) 633.

[16] S. D. Ellis and D. E. Soper, Phys. Rev. **D48**, 3160 (1993).

[17] S. D. Ellis, Z. Kunszt, and D. E. Soper, Phys. Rev. Lett. **69**, 3615 (1992).

[18] J. Huth et al., Proc. of the 1990 DPF Summer Study on High Energy Physics, Snowmass, CO, ed. by E. L. Berger (World Scientific, Singapore, 1992), p.134.

[19] P.M. Stevenson, Phys. Rev. **D23**, 2916 (1981).